H2I: A Handover-State Encoding-Based Data Inheritance Method for Mobile Crowdsensing

Haifeng Jiang[*†‡], Siyuan Yin[*†‡], Chaogang Tang[*†‡], Shuo Xiao[*†‡], Huaming Wu[§], Ruidong Li[¶]
[*]School of Computer Science and Technology, China University of Mining and Technology, Xuzhou, China
[†]Mine Digitization Engineering Research Center of the Ministry of Education, Xuzhou, China
[‡]Jiangsu Provincial Industrial Technology Engineering Center for Intelligent Sensing and Emergency IoT in Underground Space, Xuzhou, China
[§]The Center for Applied Mathematics, Tianjin University, Tianjin, China
[¶]The Institute of Science and Engineering, Kanazawa University, Kanazawa, Japan
{ts24170068P31, jhfeng, cgtang, sxiao}@cumt.edu.cn, whming@tju.edu.cn, liruidong@ieee.org

2026 IEEE/ACM International Symposium on Quality of Service (IWQoS) | 979-8-3195-1703-6/26/$31.00 ©2026 IEEE | DOI: 10.1109/IWQoS70441.2026.11661265

***Abstract*—In mobile crowdsensing (MCS), participants often drop out, requiring their unfinished tasks to be migrated to othersa process known as task migration. However, existing work rarely addresses how to properly handle the residual data from exiting participants, leading to low data utilization and degraded quality, which harms MCS Quality of Service (QoS). To tackle this, we propose H2I, a data inheritance method based on handover-state encoding. H2I first introduces a hierarchical data quality assessment framework: a point-level layer uses task-embedded multi-head attention to estimate collection quality for each record, while a grid-level layer employs an Attention U-Net to assess credibility using spatial context. These scores jointly guide data correction. We find that quality assessment alone cannot distinguish natural variations caused by task migration from true anomalies, often causing over-smoothing. To solve this, H2I incorporates handover-state encoding, which models the spatiotemporal proximity and historical observation states of the exiting participant and the successor. A gated fusion mechanism then uses this encoding to control the direction and scale of correction. Extensive simulations show that H2I outperforms existing methods in MAE, R^2, and other metrics, significantly improving data quality during task migration.**

***Index Terms*—mobile crowdsensing, data inheritance, handover-state encoding, multi-head attention, attention U-Net, gated fusion mechanism.**

I. Introduction

Driven by the rapid advancement of wireless networks and mobile terminal devices, Mobile Crowdsensing (MCS) [1] has emerged as a promising paradigm to enhance the QoS for Internet of Things (IoT) applications. It is profoundly transforming data collection in critical domains such as environmental monitoring [2]–[4], intelligent traffic systems [5]–[7], and healthcare [8], [9]. As a large-scale sensing and computing paradigm that utilizes ordinary users' smart devices as sensor nodes, MCS leverages widely distributed participants equipped with smartphones, wearables, or vehicle-mounted sensors to continuously collect environmental information like temperature, air quality, and noise. Compared to traditional fixed sensor networks, MCS offers lower costs and greater flexibility.

979-8-3195-1703-6/26/$31.00 ©2026 IEEE

However, the widespread application of MCS is fundamentally constrained by the high uncertainty in the quality of the collected sensing data, which directly dictates the provided QoS. Unlike professionally deployed sensors, MCS frequently faces the following issues: **1) Unstable data collection quality.** Since data collection is human-driven and influenced by participant-specific factors, the collected data often suffers from high volatility in quality. Consequently, techniques such as data filtering [10] are used to handle low-quality data. **2) Sparsity of mobile sensing nodes.** Insufficient numbers of participants can lead to sparse data coverage. Numerous studies have therefore focused on designing data completion algorithms [11] to fill in missing data, thereby improving the quality of the spatial sensing map. **3) Significant heterogeneity of sensing devices.** The variety of devices used by participants can result in differing data collection accuracies. When multiple device types operate in the same area, data inconsistencies can arise. This situation necessitates truth discovery algorithms [12] to determine the accurate data value for a given location.

Numerous research efforts have addressed the aforementioned three challenges. However, these studies generally assume that participants can complete their tasks normally, neglecting the scenario of task migration where a participant drops out midway and the remaining work is taken over by others. In task migration, the exiting participants may fail to complete the task on time and be removed by the system, or may abandon the task for other subjective or objective reasons. The system must then select a suitable successor to inherit and complete the task. The data partially collected by the exiting participant, if discarded directly, would result in significant data waste, severely reducing system data utilization and increasing sensing costs. Conversely, simply concatenating this data with the successors newly collected data, while maximizing data usage, can degrade overall data quality due to various differences between the two participants, thereby lowering the QoS of MCS. For instance, significant differences in device accuracy can cause abrupt data changes in adjacent areas sensed by the two participants. Moreover, task migration involves spatiotemporal shifts, breaking the continuous sensing state maintained by the exiting participant. By the time the successor begins, the environmental state in some areas may have already changed. Directly merging data from both participants would lead to semantic inconsistency, misleading data users. Therefore, a reasonable scheme is needed to properly inherit the data left by the exiting participant. Although existing work, such as that by Li et al. [13], considers inheriting the exiting participants data after task migration, their method only defines triggering conditions without addressing the overall impact of participant differences on task data quality. To date, no systematic solution has been proposed for reasonably inheriting residual data in task migration scenarios.

To address these challenges, we propose H2I (Hierarchical Handover-to-Inheritance), a novel data inheritance method for MCS under task migration. H2I evaluates data credibility through a two-level quality assessment: at the observation level, it considers collection attributes such as device noise and data freshness; at the grid level, it incorporates geospatial context. To handle participant handovers, H2I introduces a handover-state encoder that captures the exiting participants historical sensing pattern and the spatiotemporal relationship between the handover locations. The encoder produces an inheritance prior that guides a correction process to refine residual data, ensuring the final sensing output remains accurate and consistent. Unlike existing approaches that overlook the disruption caused by participant turnover, our method explicitly preserves both data quality and semantic coherence during migration. Experiments show that H2I effectively integrates residual observations from departing participants into the overall task data with superior performance. Based on the above discussion, our work makes the following contributions to improving the QoS of MCS data:

- We propose H2I, a data inheritance method for task migration scenarios. It designs a hierarchical data quality assessment mechanism and introduces the innovative concept of handover-state encoding, enabling more scientific processing and integration of the exiting participants residual data. Compared to prior studies, this work is the first to systematically design a complete data inheritance process.
- We design a task-embedded multi-head attention mechanism and an Attention U-Net to construct the point-level and grid-level quality layers, respectively. These layers evaluate observation quality from both collection quality and credibility perspectives, and the resulting scores are used for data correction. Furthermore, we propose a gated fusion mechanism guided by handover-state encoding, which injects task migration as a dynamic prior in the form of structured vectors, producing reconstructed values that better preserve physical continuity and semantic consistency.
- We evaluate H2I using real-world datasets. Experimental results show that, compared with baseline methods, H2I achieves higher-quality and more faithful sensing data.

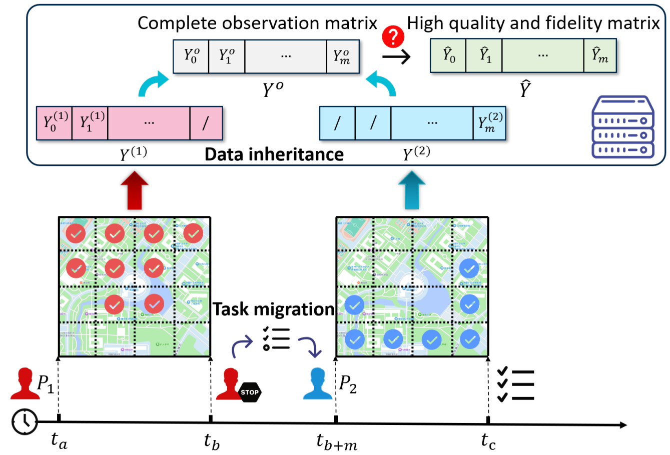

Fig. 1: Description of data inheritance issues.

II. System Model and Problem Formulation

A. System Model

As illustrated in Fig. 1, we consider a task migration scenario in a classical MCS system where a task started by participant P_1 is inherited by P_2 after a dropout. The target area is divided into I non-overlapping cells $U = \{u_1, u_2, \ldots, u_I\}$, and the total task duration is $T = T_{p_1} + T_m + T_{p_2}$. During their respective periods $T_{p_1} = [t_a, t_b]$ and $T_{p_2} = [t_{b+m}, t_c]$, participant P_1 collects data from cell subset U_1, while P_2 covers the remaining set $U_2 = U \backslash U_1$ after a migration interval $T_m = [t_b, t_{b+m}]$. Each sensing record is uploaded as a quadruple $\langle M_k, y_j^i, u_i, t\rangle$. To ensure reliability, the system selects the observation y_i for each cell whose timestamp t is closest to the task completion time t_c. The data from P_1 and P_2 form two spatially complementary, temporally disjoint observation matrices $Y^{(1)}, Y^{(2)} \in \mathbb{R}^{H\times W}$. The final observation matrix at the cloud server is represented as $Y^o = Y^{(1)} \cup Y^{(2)}$.

B. Problem Formulation

Our goal is to design a data inheritance method for task migration in MCS. We focus on how to inherit the residual observations of participant P_1 and integrate them with the sensing data collected by participant P_2. The objective is to obtain a complete sensing data matrix $\hat{Y} \in \mathbb{R}^{H\times W}$ with high quality and high fidelity. Specifically, we aim to learn a function $f(\cdot)$ that adjusts the observation matrix Y^o, which is formed by directly concatenating $Y^{(1)}$ and $Y^{(2)}$. The target matrix is obtained as $\hat{Y} = f(Y^o)$. This process enables principled inheritance of the residual data from participant P_1, rather than simply discarding or directly retaining them. The optimization objective is defined as follows:

$$\min_{f} \quad \lambda_1 \cdot \varepsilon(\hat{Y}, Y) - \lambda_2 \cdot R^2(\hat{Y}, Y), \tag{1}$$

where $\varepsilon(\cdot,\cdot)$ and $R^2(\cdot,\cdot)$ measure the accuracy and fidelity of the processed data matrix $\hat{Y}$, respectively. $\lambda_1, \lambda_2 \geq 0$ are weighting factors, and Y denotes the ground-truth data matrix.

Algorithm 1 Data Inheritance Algorithm

Input: Complete observation matrix $\mathbf{Y}^o$, grid cell set $U = \{u_1, \ldots, u_I\}$, collection attributes $\{\sigma_i, \tau_i, c_i\}$, geospatial features $\mathbf{X}^{(g)}$, handover-state features $\{y^l_{p_1}, q^N_{p_1}, T_m, d_e\}$
Output: High-quality sensing data matrix $\hat{\mathbf{Y}}$

Point-level quality layer:
for $i = 1$ to I **do**
  Normalize attributes and form $\mathbf{x}_i$
  Build task embedding $\mathbf{z}_i$ (Eq. (2))
  Compute quality score q_i via multi-head attention (Eq. (3)(4))
end for
Assemble collection quality matrix $\hat{\mathbf{Q}}$
Grid-level quality layer:
for $i = 1$ to I **do**
  Build input tensor $\mathbf{X}$ from $\mathbf{X}^{(v)}$, $\hat{\mathbf{Q}}$, Sobel($\mathbf{X}^{(v)}$), and $\mathbf{X}^{(g)}$
  Encode $\mathbf{X}$ with U-Net encoder (Eq. (5)(6))
  Enhance skip connections via Attention Gate (Eq. (7)(8))
  Decode with U-Net decoder (Eq. (9)(11))
end for
Output credibility score matrix $\hat{\mathbf{R}}$ (Eq. (12))
Data correction:
for $i = 1$ to I **do**
  Form handover-state vector $\hat{\mathbf{H}}$ from $y^l_{p_1}$, $q^N_{p_1}$, T_m, d_e
  Build main feature $\hat{\mathbf{X}}$ from $\mathbf{Y}^o$, $\hat{\mathbf{Q}}$, $\hat{\mathbf{R}}$, $\hat{\mathbf{H}}$
  Extract features to get $\mathbf{Z}'$ (Eq. (13))
  Generate gating weight $\mathbf{G}$ from $\mathbf{Y}^o$, $\hat{\mathbf{Q}}$, $\hat{\mathbf{R}}$ (Eq. (14))
  Generate bias weight $\mathbf{B}'$ from $\hat{\mathbf{H}}$ (Eq. (15))
end for
Compute corrected output $\hat{\mathbf{Y}}$ using $\mathbf{G}$ and $\mathbf{B}'$ (Eq. (16))

III. Method Design

A. Method Overview

As shown in Fig. 2, the H2I framework consists of three stages: point-level quality assessment, grid-level credibility evaluation, and handover-state encoding correction. It first generates a quality score matrix $\hat{\mathbf{Q}}$ via a task-embedded attention mechanism, then computes a grid-level credibility matrix $\hat{\mathbf{R}}$ using an attention-based U-Net to capture spatial consistency. Finally, a gated fusion module integrates handover-state encoding to reconstruct the data $\hat{\mathbf{Y}}$, ensuring semantic continuity during task migration. The complete procedure of the proposed H2I method is summarized in Algorithm 1.

B. Point-Level Quality Layer

This layer quantifies the reliability of observation y_i in cell i through a feature vector $\mathbf{x}_i = [p_i, f_i, n'_i]^\top$, where $p_i = (1 + e^{a\log(\sigma_i)-b})^{-1}$ models device noise σ_i, $f_i = (1 + e^{\tau_i/L_v})^{-1}$ reflects data freshness via age τ_i, and $n'_i = \log(1+c_i)/\log(1+c_r)$ normalizes the observation frequency c_i (as shown in Fig. 3). To handle varying sensitivities across task types (e.g., PM2.5 vs. temperature), we employ a task-embedded multi-head attention mechanism.

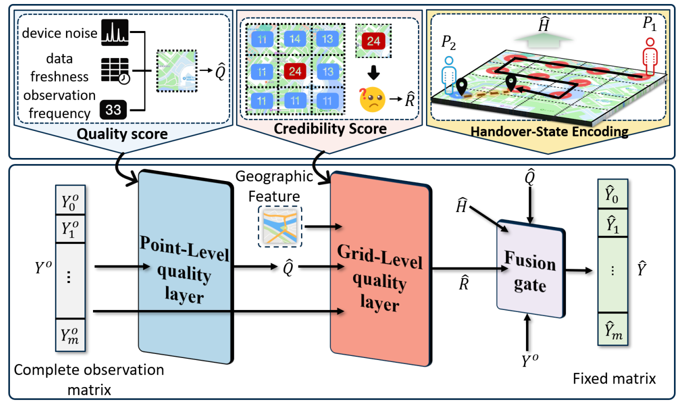

Fig. 2: Structure of H2I data inheritance method.

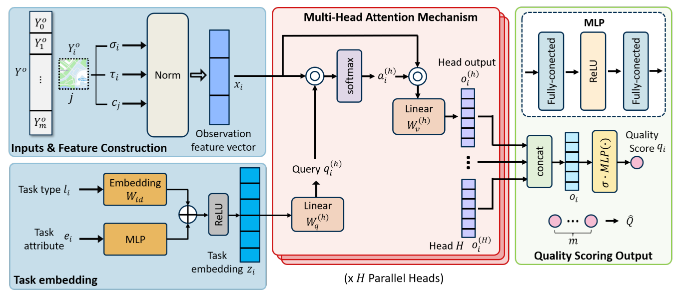

Fig. 3: Structure of point-level quality layer.

We first construct a task embedding $\mathbf{z}_i$ by fusing task IDs and prior attributes:

$$\mathbf{z}_i = \mathrm{ReLU}(W_{\mathrm{id}}[l_i] + \mathrm{MLP}(\mathbf{e}_i)) \tag{2}$$

where W_{id} denotes the learnable embedding lookup table, d_t is the embedding dimension, and $e_i = [\tilde{n}_i, \tilde{f}_i, \tilde{s}_i]^\top \in \mathbb{R}^F$ represents the prior attributes of task i. Specifically, $\tilde{n}_i$ is the maximum allowable noise level, $\tilde{f}_i$ is the data lifetime constraint, and $\tilde{s}_i$ represents the minimum required number of observations for the task. For each head h, the task embedding modulates the features via element-wise multiplication ($\odot$) to capture task-specific preferences:

$$\mathbf{a}_i^{(h)} = \mathrm{softmax}\left(\frac{(W_q^{(h)}\mathbf{z}_i) \odot \mathbf{x}_i}{\sqrt{F}}\right) \tag{3}$$

$$\mathbf{o}_i^{(h)} = W_v^{(h)}(\mathbf{a}_i^{(h)} \odot \mathbf{x}_i) \tag{4}$$

The final quality score $q_i \in [0, 1]$ is predicted by an MLP with sigmoid activation: $q_i = \sigma(\mathrm{MLP}(\mathrm{concat}(\mathbf{o}_i^{(1)}, \ldots, \mathbf{o}_i^{(H)})))$. This reweighted representation allows the model to dynamically prioritize features based on the specific sensing context.

C. Grid-Level Quality Layer

To prevent local anomalies from degrading the sensed matrix, we evaluate the credibility of each grid cell within its spatial context. Unlike traditional CNN or FCN that may lose fine-grained details, we employ an Attention U-Net to fuse multi-scale information. Its symmetric encoder-decoder structure with skip connections allows the model to distinguish between natural geographic variations and artificial noise. The

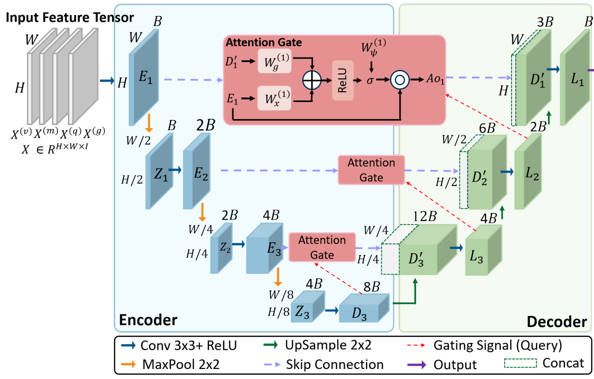

Fig. 4: Structure of grid-level quality layer.

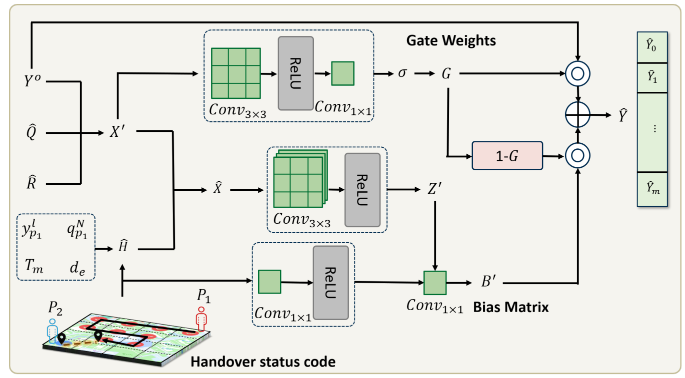

Fig. 5: Description of data correction process.

architecture is illustrated in Fig. 4.

1) Feature Tensor Construction: The input tensor $\mathbf{X} = [\mathbf{X}^{(v)}, \mathbf{X}^{(m)}, \mathbf{X}^{(q)}, \mathbf{X}^{(g)}] \in \mathbb{R}^{H \times W \times I}$ integrates observed values, spatial gradients (via Sobel operator), point-level quality scores $\hat{\mathbf{Q}}$, and geographic context features (e.g., building blockages or traffic hubs).

2) Encoder: The encoder extracts multi-scale features through downsampling. For each layer k, it computes features $\mathbf{E}_k$ and downsampled maps $\mathbf{Z}_k$:

$$\mathbf{E}_k = \mathrm{ReLU}(\mathrm{Conv}_{3\times3}(\mathbf{Z}_{k-1})) \tag{5}$$

$$\mathbf{Z}_k = \mathrm{MaxPool}_{2\times2}(\mathbf{E}_k) \tag{6}$$

where $\mathbf{E}_k$ represents the feature map at layer k, and $\mathbf{Z}_k$ is the downsampled input for the next layer.

3) Attention Gate: Standard skip connections treat all spatial locations equally. We introduce Attention Gates at each skip connection to dynamically enhance relevant regions using a spatial weight map $\boldsymbol{\psi}_k$ derived from the decoder state $\mathbf{D}'_{k+1}$ and encoder features $\mathbf{E}_k$:

$$\boldsymbol{\psi}_k = \sigma(W\psi(\mathrm{ReLU}(W_g\mathbf{D}'_{k+1} + W_x\mathbf{E}_k))) \tag{7}$$

$$\mathbf{Ao}_k = \mathbf{E}_k \odot \boldsymbol{\psi}_k \tag{8}$$

where $\boldsymbol{\psi}_k$ denotes the attention weights, and $\mathbf{Ao}_k$ represents the modulated features.

4) Decoder and Output: The decoder restores spatial resolution while merging fine-grained details:

$$\mathbf{D}'_k = \mathrm{UpSample}_{2\times2}(\mathbf{D}_k) \tag{9}$$

$$\mathbf{M}_k = \mathrm{Concat}(\mathbf{D}'_k, \mathbf{Ao}_k) \tag{10}$$

$$\mathbf{L}_k = \mathrm{ReLU}\left(\mathrm{Conv}_{3\times3}(\mathbf{M}_k)\right) \tag{11}$$

where $\mathbf{D}'_k$ is the upsampled state, and $\mathbf{M}_k$ is the fused feature map. The final credibility matrix $\hat{R}$ is obtained as:

$$\hat{R} = \sigma(\mathrm{Conv}_{1\times1}(\mathbf{L}_1)) \in [0,1]^{H\times W}. \tag{12}$$

D. Data Correction

While $\hat{\mathbf{Q}}$ and $\hat{\mathbf{R}}$ reflect static spatiotemporal snapshots, they fail to capture the dynamic effects caused by participant handover, which can lead to data discontinuity. To address this, we propose a handover-state encoding mechanism and a Fusion Gate to balance raw observations with context-aware reconstruction. The overall data correction process is illustrated in Fig. 5. We first construct a static feature tensor $\mathbf{X}' = [\mathbf{Y}^o, \hat{\mathbf{Q}}, \hat{\mathbf{R}}] \in \mathbb{R}^{H\times W\times 3}$ and a handover-state vector $\hat{\mathbf{H}} = [y^l_{p_1}, q^N_{p_1}, T_m, d_e]^\top$. Here, $\hat{\mathbf{H}}$ explicitly captures the last observation, historical quality, handover time, and geographic distance between exiting and incoming participants to serve as a dynamic transition prior. To extract deep spatial context, we define the main trunk features $\mathbf{Z}'$ based on the combined tensor $\hat{\mathbf{X}} = [\mathbf{Y}^o, \hat{\mathbf{Q}}, \hat{\mathbf{R}}, \hat{\mathbf{H}}]$:

$$\mathbf{Z}' = \mathrm{ReLU}\left(\mathrm{Conv}^{(3)}_{3\times3}(\hat{\mathbf{X}})\right) \tag{13}$$

where $\mathbf{Z}'$ represents the features extracted through three consecutive convolutional layers. Simultaneously, a gating matrix $\mathbf{G}$ is computed to determine the blending weights between original data and model reconstruction:

$$\mathbf{G} = \sigma\left(\mathrm{Conv}_{1\times1}\left(\mathrm{ReLU}(\mathrm{Conv}_{3\times3}(\mathbf{X}'))\right)\right) \tag{14}$$

where $\mathbf{G} \in [0,1]^{H\times W}$ is the gating weight, and σ is the sigmoid function. The bias branch $\mathbf{B}'$ is then generated by fusing the spatial trunk features with the handover-state encoding:

$$\mathbf{B}' = \mathrm{Conv}_{1\times1}\left(\left[\mathbf{Z}',\ \mathrm{ReLU}\left(\mathrm{Conv}_{1\times1}(\hat{\mathbf{H}})\right)\right]\right) \tag{15}$$

where $\mathbf{B}'$ contains the specific correction bias for each grid cell. Finally, the complete corrected sensing matrix $\hat{\mathbf{Y}}$ is produced via a gated fusion mechanism:

$$\hat{\mathbf{Y}} = \mathbf{G} \odot \mathbf{Y}^o + (1 - \mathbf{G}) \odot \mathbf{B}' \tag{16}$$

where $\odot$ denotes element-wise multiplication. This formulation ensures that the system relies more on $\mathbf{B}'$ in handover-affected or low-quality regions, while preserving reliable original observations $\mathbf{Y}^o$ where the gating weight $\mathbf{G}$ is high.

IV. Simulation Experiments

A. Experimental Setup

To verify the proposed method, we conduct simulation experiments using two public datasets: *UrbanAirNet*[1] (extracting PM2.5, temperature, and wind speed) and *COTS 5G*[2]

[1]https://www.kaggle.com/ziya07/datasets?query=urbanairnet
[2]https://www.kaggle.com/datasets/samiemostafavi/wireless-pr3d

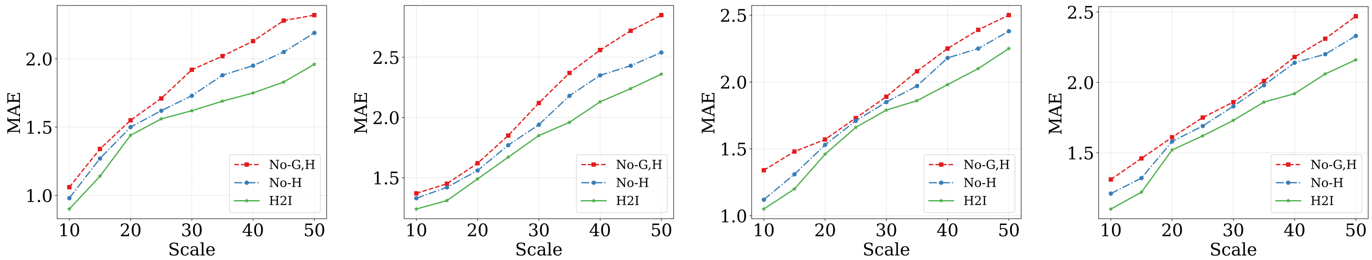

(a) PM2.5 (b) Temperature (c) RSRP (d) WindSpeed

Fig. 6: MAE performance on different datasets with varying data scales.

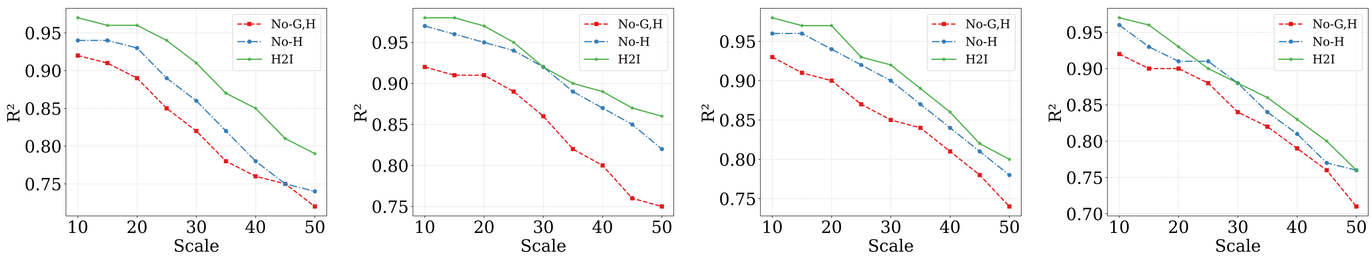

(a) PM2.5 (b) Temperature (c) RSRP (d) WindSpeed

Fig. 7: R^2 performance on different datasets with varying data scales.

(extracting RSRP). The monitored area is modeled as a 20×20 grid. To simulate real-world conditions, we introduce different levels of device noise and change values in random cells to model special geographic features. The sensing data are split by time to represent separate collection phases before and after task handover. The model is implemented in TensorFlow using the Adam optimizer and trained on an NVIDIA Tesla A100 PCIe GPU (CentOS 7, CUDA 11.5, cuDNN 8.6).

B. Ablation Study

In this section, we conduct ablation experiments on the proposed data inheritance method (H2I) to verify the contribution of each core component to the overall performance. For the H2I method, we design the following four ablation variants:

- **No-P,G,H:** The observation matrix is obtained by directly merging the data from the two participants and used as the target sensing data matrix.
- **No-G,H:** Uses only point-level quality scores for correction; removes the grid-level layer and handover-state encoding.
- **No-H:** Uses the full hierarchical quality assessment but excludes handover-state encoding.
- **H2I:** The complete method with both hierarchical quality assessment and handover-state encoding.

We first conduct ablation studies on 20×20 observation matrices across four physical quantities. To evaluate scalability, we tested varying data scales (Fig. 6, 7). While performance gains for all methods diminish at larger scales due to environmental heterogeneity, the H2I model maintains superior stability. Specifically, versions lacking spatial context (No-G,H) or handover modeling (No-H) suffer from significant degradation or over-smoothing. By explicitly modeling the handover-state to guide correction, H2I effectively preserves legitimate data variations across all scales.

C. Comparative Experiments

To validate the advantages of the proposed H2I method, we compare it against four baseline methods: **WA** [14], which learns a context-dependent scaling factor; **AER** [15], an encoder-decoder structure for truth reconstruction; **GAN** [16], an adversarial framework for generating realistic results; and **STE-STA**, a fully connected network learning a unified correction mapping. To test resilience to handover durations, we varied the interval T_m (Fig. 8, 9). Although all methods degrade as T_m increases, H2I exhibits the slowest performance drop. This stability is attributed to its handover-state encoding mechanism, which leverages the previous participants exit state as a prior to maintain high-quality data inheritance even after long temporal gaps.

V. Conclusion

In this paper, we propose H2I, a data inheritance method for MCS that uses handover-state encoding. H2I includes a two-level quality assessment: a point-level layer that estimates data quality using device noise, freshness, and observation frequency via multi-head attention, and a grid-level layer that evaluates spatial credibility using an Attention U-Net. We also introduce a handover-state encoding mechanism to explicitly model participant transitions during task handover. These quality scores jointly guide the correction of inherited data. Experiments on multiple datasets show that H2I produces higher-quality sensing matrices than simply combining data

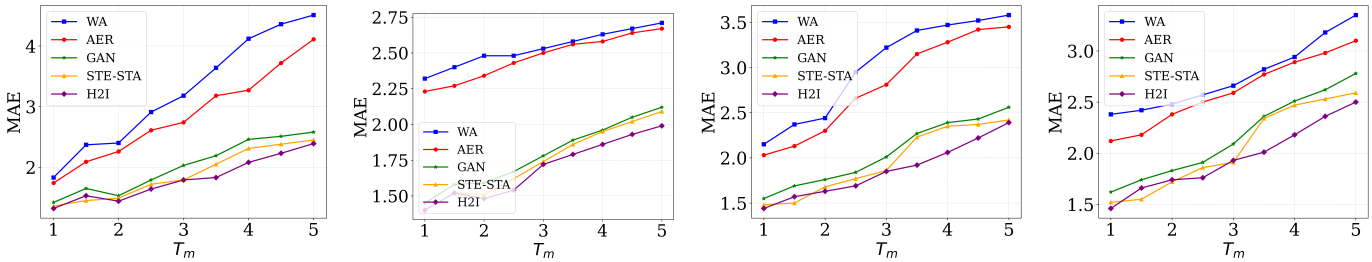

(a) PM2.5 (b) Temperature (c) RSRP (d) WindSpeed

Fig. 8: MAE performance on different datasets with varying T_m.

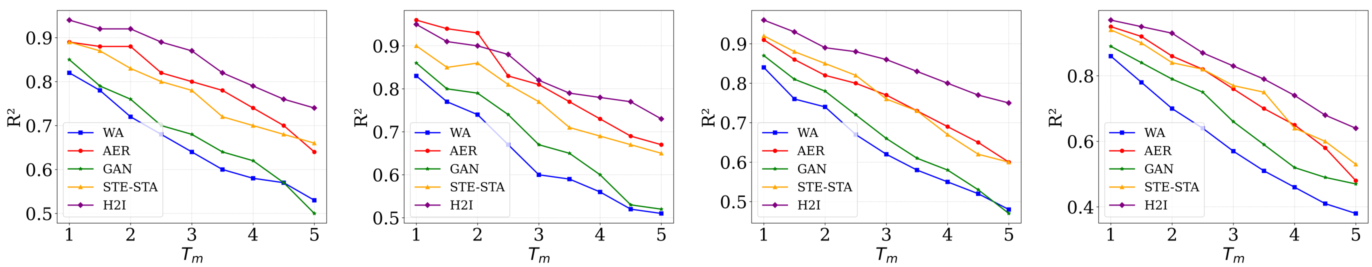

(a) PM2.5 (b) Temperature (c) RSRP (d) WindSpeed

Fig. 9: R^2 performance on different datasets with varying T_m.

from two participants or using existing baseline methods. For future work, we aim to address the cold-start problem. Current H2I relies on abundant historical data, but real-world handovers often occur with little prior experience. We plan to develop approaches that enable fast adaptation from only a few handover examples.

ACKNOWLEDGMENT

This work was supported in part by the National Natural Science Foundations of China under Grant 62476276 and Grant 62271486.

REFERENCES

[1] R. K. Ganti, F. Ye, and H. Lei, "Mobile crowdsensing: Current state and future challenges," *IEEE Commun. Mag.*, vol. 49, no. 11, pp. 32–39, Nov. 2011.

[2] J. Zhang, L. Han, and B. Guo, "Sparse mobile crowdsensing for gas monitoring in coal mine working face," *IEEE Internet Things J.*, vol. 11, no. 22, pp. 36633–36645, Nov. 2024.

[3] J. Rubio-Aparicio and J. Santa, "An embedded crowdsensing unit for mobile urban pollution monitoring," *IEEE Commun. Mag.*, vol. 61, no. 1, pp. 90–96, Jan. 2023.

[4] J. Zhang, Q. Yan, X. Zhu, and K. Yu, "Smart industrial IoT empowered crowd sensing for safety monitoring in coal mine," *Digit. Commun. Netw.*, vol. 9, no. 2, pp. 296–305, Apr. 2023.

[5] R. Huang, L. Cheng, Z. Li, C. Xiang and Y. Guo, "iPatrol: Illegal roadside parking detection leveraging on-road vehicle crowdsensing," *in Proc. IEEE Int. Workshop Qual. Serv. (IWQoS)*, Guangzhou, China, 2024, pp. 1-10.

[6] M. Li, M. Ma, L. Wang, B. Yang, T. Wang, and J. Sun, "Multitask-oriented collaborative crowdsensing based on reinforcement learning and blockchain for intelligent transportation system," *IEEE Trans. Ind. Inform.*, vol. 19, no. 9, pp. 9503–9514, Sept. 2023.

[7] M. Li, M. Ma, L. Wang, Z. Pei, J. Ren, and B. Yang, "Multiagent deep reinforcement learning based incentive mechanism for mobile crowdsensing in intelligent transportation systems," *IEEE Syst. J.*, vol. 18, no. 1, pp. 527–538, Mar. 2024.

[8] K. Rezaee, M. R. Khosravi, H. Attar, V. G. Menon, M. A. Khan, and H. Issa, "IoMT-assisted medical vehicle routing based on UAV-borne human crowd sensing and deep learning in smart cities," *IEEE Internet Things J.*, vol. 10, no. 21, pp. 18529–18536, Nov. 2023.

[9] T. Shou, Z. Ye, Y. Hong, Z. Wang, H. Zhu, Z. Jiang, D. Yang, B. Zhou, C. Wang, and L. Chen, "CrowdQ: Predicting the queue state of hospital emergency department using crowdsensing mobility data-driven models," *in Proc. ACM Interact., Mobile, Wearable Ubiquitous Technol.*, vol. 7, no. 3, pp. 1–28, Sept. 2023.

[10] Y. Zhang, J. Xu, and X. Liu, "Privacy-preserving traffic violation image filtering and searching via crowdsensing," *Mobile Netw. Appl.*, vol. 27, pp. 1–28, Apr. 2022.

[11] X. Kang, S. Tian, F. Kou, L. Shi, and J. Ren, "StrucFormer: Structural prior guided transformer for mobile crowdsensing data inference," *in Proc. ICASSP IEEE Int. Conf. Acoust., Speech Signal Process. (ICASSP)*, Hyderabad, India, 2025, pp. 1–5.

[12] J. Xiao, H. Li, H. Jiang, S. Liu, Y. Zhao, and Y. Ren, "Uncertainty-aware cross-graph learning for conflicting data truth inference in vehicular crowdsensing," *IEEE Trans. Netw. Sci. Eng.*, vol. 13, pp. 2741–2759, Oct. 2025.

[13] H. Li, Z. Yu, and Y. Luo, "ContinuousSensing: A task allocation algorithm for humanrobot collaborative mobile crowdsensing with task migration," *CCF Trans. Pervasive Comput. Interact.*, vol. 6, no. 3, pp. 228–243, Sept. 2024.

[14] Y. Li, J. Gao, P. P. C. Lee, L. Su, C. He, F. Yang, and W. Fan, "A weighted crowdsourcing approach for network quality measurement in cellular data networks," *IEEE Trans. Mob. Comput.*, vol. 16, no. 2, pp. 300–313, Feb. 2017.

[15] C. Liu, Y. Zhao, K. Zhu, S. Zhang, and J. Wu, "Cost-effective signal map crowdsourcing with auto-encoder based active matrix completion," *in Proc. IEEE 25th Int. Conf. Parallel Distrib. Syst. (ICPADS)*, Tianjin, China, 2019, pp. 761–768.

[16] Y. Zhao, C. Liu, K. Zhu, S. Zhang, and J. Wu, "GSMAC: GAN-based signal map construction with active crowdsourcing," *IEEE Trans. Mob. Comput.*, vol. 22, no. 4, pp. 2190–2204, Apr. 2023.